

Air Plasma Assisting Microcontact Deprinting and Printing for Gold Thin Film and PDMS Patterns

Hong-Lei Gou, Jing-Juan Xu, Xing-Hua Xia, and Hong-Yuan Chen*

Key Laboratory of Analytical Chemistry for Life Science, School of Chemistry and Chemical Engineering, Nanjing University, Nanjing 210093, China

ABSTRACT In this paper, we present a simple method to fabricate gold film patterns and PDMS patterns by air plasma assisting microcontact deprinting and printing transfer approaches. Chemical gold plating is employed instead of conventional metal evaporation or sputtering to obtain perfect gold film both on flat and topographic PDMS chips, and complicated SAM precoating is replaced by simple air plasma treatment to activate both the surface of gold film and PDMS. In this way, large area patterns of conductive gold film and PDMS patterns could be easily obtained on the elastomeric PDMS substrate. Both the chemical plating gold film and transferred gold film were of good electrochemical properties and similar hydrophilicity with smooth and conductive surface, which made it potentially useful in microfluidic devices and electronics. The gold transfer mechanism is discussed in detail. For typical applications, a cell patterning chip based on the gold pattern was developed to imply the interfacial property, and dielectrophoresis control of live cells was carried out with the patterned gold as interdigital electrodes to show the conductivity.

KEYWORDS: microcontact deprinting • transfer printing • gold film • pattern • dielectrophoresis • cell

INTRODUCTION

Micro- and nanosized metal patterns on various substrates are widely used in many research fields such as physics, chemistry, biology, electronics, and photonics. Various devices can be fabricated, including MEMS device, biodevice, plastic electronics, flexible display, and so on. Currently, two standard methods commonly used for metal patterning are photolithography and E-beam lithography. They typically require the use of sacrificial resists, metal deposition or sputtering, etching procedures or post patterning deposition steps. Although conventional photolithography techniques have been continuously improved, high capital investments and running costs are still obstacles for many researchers to use it in their research. Furthermore, photolithography systems are usually for large wafer sizes only, and may not be facilely used in ordinary laboratories with a variety of different purposes or requirements. E-beam lithography is a good choice when the pattern reaches submicrometer dimensions; however, it requires elaborate and expensive systems, which are capable of patterning only a narrow range of materials over small areas on ultraflat rigid substrates, thus making the final products either limited to a small area size or very time-consuming and expensive. With these limitations, substantial interest has been created in the alternative techniques, such as the method known as microcontact printing (μ -CP), which belongs to the family of soft lithography techniques

(1) developed by Whitesides and co-workers, is rapidly becoming an important method for a series of applications in micro/nano fabrication (2–4), biotechnology (5, 6) and plastic electronics (7–10). This method offers fast and low-cost approaches for patterning flat or curved surfaces over large areas in a single processing step, which meets the requirements of patterning that cannot be satisfied easily with conventional methods.

The transfer printing (11–17) is an extension of the microcontact printing technique. This new form of microcontact printing is a useful technique for many areas, such as electronics, photonics, and fluidics. In this technique, either a soft or a hard material can be used as a mold, and specific covalent interactions guide the transfer of the materials from stamps to substrates. While with a topographic stamp transferring materials from substrates, the process can be seen as “deprinting” (18). However, in most of the cases (19–22), a self-assembly monolayer (SAM) with thiol groups oriented upward must be prepared ahead to serve as covalent “glues” and “release” layer for the transfer. Although the technique had been improved a lot since it was established, the use of metal sputtering machine and complicated SAM coated step limited its application in ordinary chemistry laboratories.

In this paper, we introduced an electroless plating method to replace the conventional metal sputtering to form a perfect gold film (23, 24), and employed microcontact deprinting and transfer printing to fabricate elaborate gold patterns and PDMS patterns, both on elastomeric PDMS which had been seldom reported. Moreover, we used air plasma instead of complicated SAM coating process to activate the surface and to form covalent bond between

* Corresponding author. Tel./Fax: +86-25-83594862. E-mail: hychen@nju.edu.cn.

Received for review November 21, 2009 and accepted April 9, 2010

DOI: 10.1021/am100196z

2010 American Chemical Society

PDMS and gold. Meanwhile, we have prepared two gold patterns by this way for cell patterning and dielectrophoresis control of live cells to illustrate the potential applications of the transfer method.

EXPERIMENTAL SECTION

Material and Reagents. Sylgard 184 (including PDMS monomer and curing agent) was purchased from Dow Corning (Midland, MI). H-Arg-Gly-Asp-Cys-OH (RGDC) peptide was synthesized by GenScript (NJ, USA). Acridine Orange (AO) was from Amresco (Solon, OH). $\text{HAuCl}_4 \cdot 4\text{H}_2\text{O}$ was from Shanghai Chemical Reagent Co., Ltd. (Shanghai, China). Glucose and mannitol was from Shanghai Bio Life Science & Technology Co., Ltd. (Shanghai, China). Glass plates coated with chromium and photoresist for chip fabrication were obtained from Shaoguang Microelectronics Crop. (Changsha, Hunan, China). All other chemicals were of analytical grade and used without further purification. Milli-Q grade water (Millipore Inc., Bedford, MA) was used for all solutions and cleaning steps. The buffer was 10 mM phosphate-buffered saline (PBS, pH 7.4) containing 137 mM NaCl, 2.7 mM KCl, 87.2 mM Na_2HPO_4 , and 14.1 mM KH_2PO_4 . Dielectrophoresis solution was a buffer solution (pH 7.4) containing 250 mM mannitol, 10 mM HEPES, 15 mM K_3PO_4 , and 1 mM MgCl_2 .

Fabrication of PDMS Chip with Positive and Negative Patterns. Traditional photolithography and wet chemical etching technique were used to make microfluidic glass chips with different micropatterns. The glass plate was exposed to UV radiation under a mask with designed micropatterns, followed by developing with 0.5% NaOH solution and etching with 1 M HF/ NH_4F solution. After that, glass chips with corresponding negative patterns were obtained. On the basis of glass chips, degassing PDMS were casted and cured to replicate the patterns for positive ones, which would be served as templates for a second replication to obtain PDMS chips with the same positive patterns.

Fabrication of Gold Film on PDMS Chip. Flat gold films were fabricated on flat PDMS chips with the method described detailedly in our previous work (23), and topographic gold films were obtained with the same way just replacing the flat “cover PDMS chips” with positive or negative patterned ones. In brief, the named chemical gold plating method was pursued with a mixture solution containing 1% (w/v) HAuCl_4 , 200 g L^{-1} KHCO_3 , and 2% (w/v) glucose (v/v, 2:1:1) confined in a poly(methyl methacrylate) (PMMA) frame by two native PDMS chips. In this work, only the cover chips with gold film were employed. To reduce the defects induced by air bubbles adhering with the cover chips, the solution should be injected into the sandwich architecture after sometime when the color turned into a little dark.

Gold Film Patterning and PDMS Patterning. Patterning with Flat Gold Film. Flat PDMS chips with gold film and stamp PDMS chips with negative and positive patterns were treated with air plasma for 100s at the same time, followed by immediate contact with each other. After 5 min in 60 °C, PDMS chips were peeled off the gold film substrates. The parts of the gold films contacting with the PDMS were then adhered and peeled off, and thus the left areas with corresponding patterns were achieved, which showed positive gold patterns used negative stamps while negative PDMS patterns used positive ones. This process is called the “deprinting” process.

Patterning with Topographic Gold Film. In this part, positive and negative patterned PDMS chips with gold film served as stamp chips. After the same treatment mentioned above, positive or negative stamp chips were imprinted on flat PDMS chips in a “printing” way, which led to gold film being transfer-

printed on the substrates to form positive gold patterns or negative PDMS patterns while being peeled off the flat PDMS chips.

Cell Patterning. For grafting a multipetide RGDC on gold efficiently, flat PDMS substrates with gold film patterns were immersed overnight in 50% ethanol containing 2 mM RGDC. Unreacted RGDC was removed from the substrates by rinsing with 50% ethanol subsequently. Human liver carcinoma (from Gulou Hospital, Nanjing, China) were maintained in Dulbecco's Modified Eagle Media (DMEM, Gibco Invitrogen Corp., USA) supplemented with 10% fetal bovine serum (Gibco Invitrogen Corp., USA) at 37 °C and 5% CO_2 environment. Confluent SMMC-7721 cells were trypsinized, washed, and then resuspended in DMEM supplemented with 10% fetal bovine serum, and directly seeded on the RGDC-grafted PDMS substrates at a density of ca. 5×10^5 cells mL^{-1} . After incubation for 2 h, the substrates were washed with PBS moderately and observed with a microscope. AO staining was used for fluorescence observation.

Dielectrophoresis Control. For dielectrophoresis control, comb gold patterns were made and led as interdigital electrodes to apply an ac signal. A PDMS spacer was then constructed on the electrodes area. Human promyelocytic leukemia cells (HL-60, from Gulou Hospital, Nanjing, China) were maintained in the same condition as above. Confluent HL-60 cells were washed and resuspended in dielectrophoresis solution, and then pipetted into the chamber. A 10 V peak-to-peak alternating current (AC) electric field was supplied by a function generator at 10 kHz frequency.

Imaging and Image Analysis. DMIRE2 Inverted fluorescence microscope (Leica, Germany) equipped with DP71 CCD (Olympus, Japan) was used for microimaging (bright-field, phase contrast and fluorescent images). Image-Pro Plus (IPP) software was employed for image analysis. Photos were acquired by using a Nikon camera 4300.

Instruments. Images of scanning electron micrographs (SEM) were performed on Hitach S-4800 field emission scanning electron microscope (Hitach, Japan) at an accelerating voltage of 5 kV. X-ray photoelectron spectroscopy (XPS) measurement was taken with a Thermo ESCALAB 250 (Thermo, USA) equipped with a monochromatic Al $\text{K}\alpha$ source operated at 150 W. A CAM 200 contact angle goniometer (KSV Instruments Ltd., Helsinki, Finland) was used to measure water contact angles. Electrochemical measurements were performed on a CHI 750C electrochemical workstation (Shanghai Chenhua Apparatus Corp., China), with a Pt auxiliary electrode and a homemade Ag/AgCl reference electrode. Dielectrophoresis control by an AC signal was carried out with a function generator (XD-2, Jiangsu Hongze Electronic Equipment Corp., China).

RESULTS AND DISCUSSION

Transfer of the Gold Film and Characterization.

Recently, an electroless plating method was developed to prepare gold films on the surfaces of PDMS chips by our group (23, 24). Both PDMS chips, named the cover chip and the base chip, were coated with a gold film simultaneously via electroless plating with the help of a sandwich-typed framework (Figure 1). A one-layer smoothly structured gold film is presented on the cover chip, whereas a two-layer structured film comprising a tight layer and a loose layer is obtained on the base chip. This method could also be used to fabricate topographic gold film. By replacing the flat PDMS chip with a topographic PDMS chip, which has positive or negative patterns of channels, graphics, and characters, we can achieve topographic gold films over the corresponding patterns on PDMS chips as well. To get a good transfer,

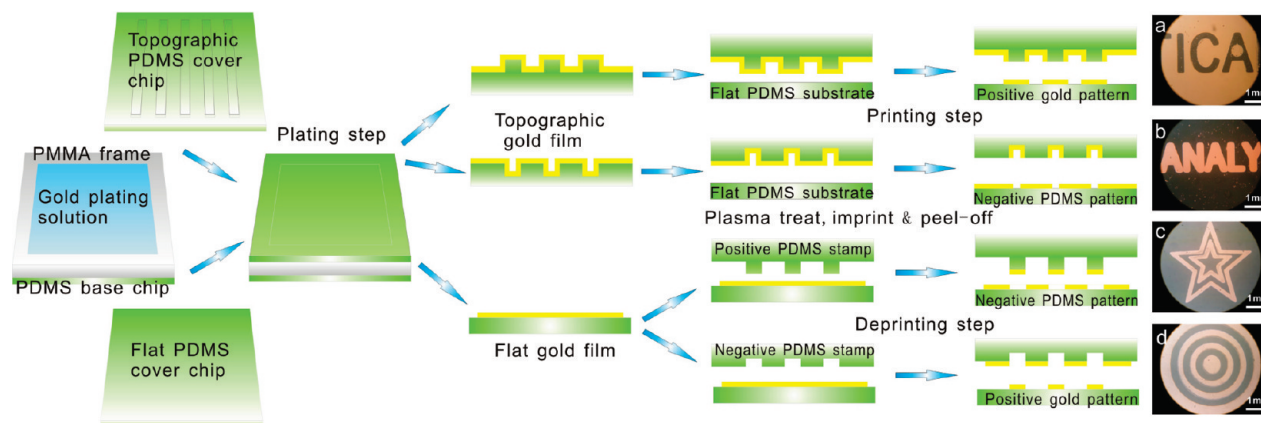


FIGURE 1. Schematic diagram of the whole processes for the formation of gold film patterns and PDMS patterns.

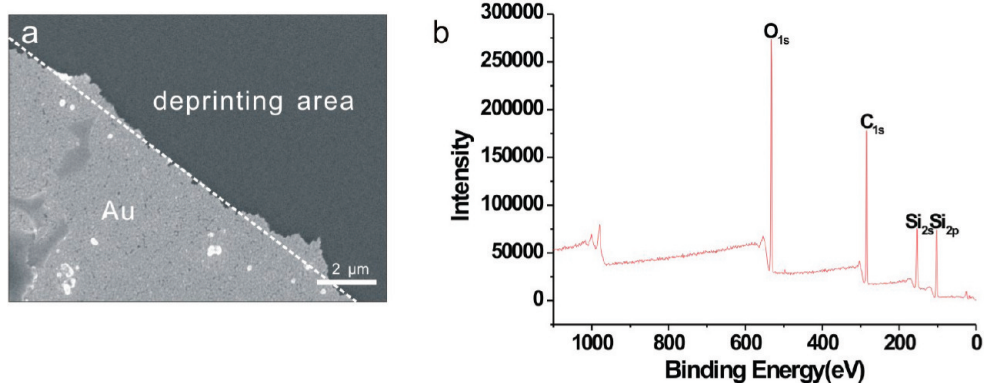


FIGURE 2. (a) SEM of the boundary area of gold pattern and (b) XPS of the deprinting area.

smooth surfaces of the gold film and PDMS stamp were essential to ensure close contact between the gold film and PDMS stamp. Thus, the cover chip with a smooth gold film was employed to make the transfer and patterns. The whole processes have been shown in Figure 1. By imprinting the positive gold film as stamp on a flat PDMS, the raised parts of the film would contact and adhere with the PDMS, and thus positive gold patterns would be printed on the substrate after peel-off (Figure 1a). While using the negative gold film as stamp, the whole film would be transferred on the substrate except the sunken parts over the negative patterns, which made the PDMS exposed to form negative patterns (Figure 1b). Likewise, on the flat gold film, when imprinting a positive PDMS mold, contacting parts of the gold would be deprinted away from the substrate to form PDMS patterns among the bulk gold film (Figure 1c). With a negative PDMS stamp, contactless parts of the gold would be reserved while the other parts would be peeled off to make positive gold patterns (Figure 1d).

Gold transfer effect was investigated by SEM and XPS of the deprinting area. A perfect transfer of the gold film would make a clean PDMS area exposed. Figure 2a implies that, after peel-off, the gold of the contacting area was transferred away by the stamp, leaving the desired gold pattern on the substrate, and that the boundary fluctuation was less than 1 μm . Figure 2b showed the XPS results of the deprinting area. Only the peaks of O_{1s} , C_{1s} , Si_{2s} , and Si_{2p} come from PDMS substrate were found and no typical peaks of gold

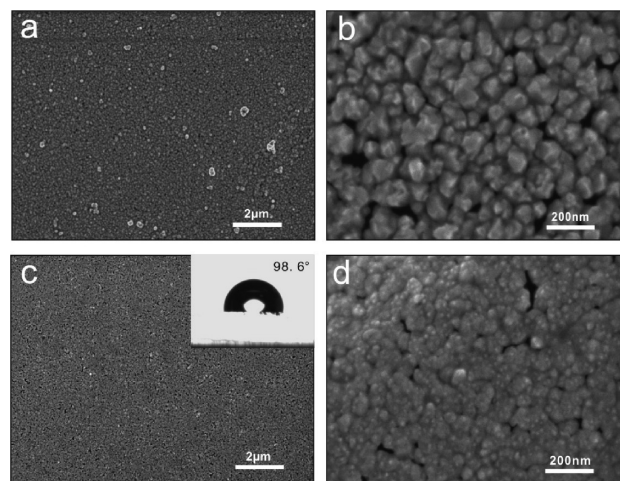


FIGURE 3. SEM of (a, b) original gold film and (c, d) transferred gold film.

appeared, which meant gold film contacting with the stamp was fully deprinted away from the PDMS substrate (Figure 2b).

The surface properties of the original gold film and transferred gold film were investigated by SEM, water contact angle measurements, and cyclic voltammetry (CV). SEM images showed that the smooth original gold layer on cover chip was a continuous layer due to the adsorption of the nanoparticles in the deposition step (Figure 3a). By magnification image (Figure 3b), we found that it was fabricated by irregular and angular gold nanoparticles about

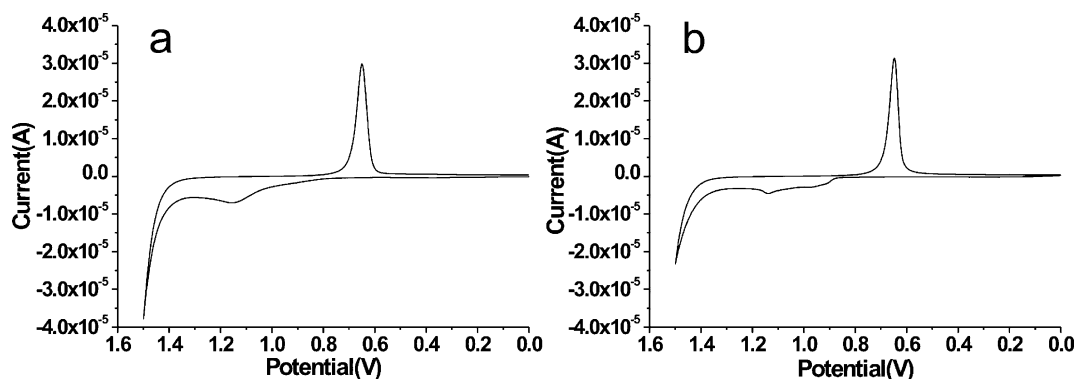


FIGURE 4. Cyclic voltammogram of (a) original gold film and (b) transferred gold film in 0.5 M H_2SO_4 . Scan rate is 50 mV s^{-1} .

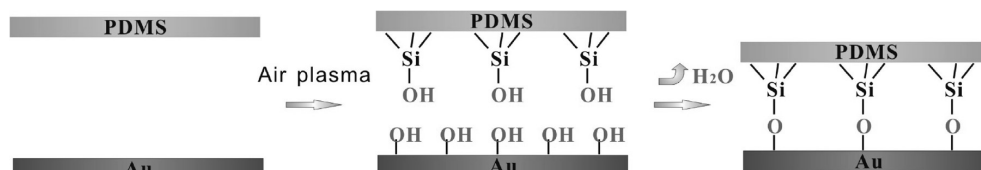


FIGURE 5. Adhesion mechanism of the plasma-assisted transfer.

100 nm, which distributed and accumulated with each other to form a compact layer. When being transferred, the gold film was reversed and the original underside was exposed. Compared to that of the original gold film, SEM images of the transferred gold film showed a more compact and smooth surface (Figure 3c). And on the surface (see Figure 3d, magnification), a lot of ca. 10 nm sized gold nanoparticles were obviously observed, which were speculated as the catalytic centers synthesized in situ through the electroless plating on PDMS. It would be an obvious proof for the fabrication mechanism of the gold film described in our previous work (23). That is, the residual Si–H in PDMS directly reduced HAuCl_4 to produce gold nanoparticles on the surface even in the matrix of the PDMS, which acted as seeds to induce gold deposition on PDMS in the reduction of HAuCl_4 by glucose and form a continuous gold layer.

The chemical plating gold film took on a good conductivity and a typical electrochemical behavior by CV scan in 0.5 M H_2SO_4 within a 1.5 mm hole confined in PDMS, which meant it could fabricate gold film electrode or band electrode for specific use (Figure 4a). With the property, electrochemical etching for gold pattern (23) and nanoband electrode for microfluidic detection (25) were carried out in our previous work. When being transferred, the gold film reserved the conductivity and electrochemical properties. The CV curves showed typical electrochemical properties that are similar to that of the original gold film (Figure 4b), with a close calculated surface roughness factor of 2.66 for transferred gold film and 2.23 for original gold film. The slight increase of R_f might derive from the plenty of tiny nanoparticles on the surface of transferred gold film. And the transferred film had a similar hydrophilic property with a water contact angle of 98.6° (Figure 3c insert), which was a little lower than that of the original one. The small difference of water contact angle might result from that, the surface of the transferred gold film was a little more compact and flat than that of the

original gold film, which could be seen clearly comparing images b and d in Figure 3.

Transfer Mechanism of Gold Film. To the best of our knowledge, in most literature related to the transfer of gold film or gold nanoparticles, chemicals such as thiol terminated xysilane to strengthen the bonding between PDMS and gold were commonly used (19–22). But few referred to the direct transfer of gold. Recently, many reports described that, after ultrahigh vacuum, electron bombardment, UV/ozone, or plasma treatment, atomic oxygen were adsorbed on the gold surface (26–34). Our group also found that after air plasma treatment, $\text{Au}(\text{OH})_x$ was generated on the surface of chemical plating gold film (24). Actually, they do not conflict at all. Because of the intense activity of adsorbed atomic oxygen, it will react very quickly with the water when exposed in air (28, 35). Therefore, $-\text{OH}$ groups will generate on the gold surface. When plasma-treated stamp PDMS was imprinted on the gold film, Si–OH on PDMS and $-\text{OH}$ on gold would link and dehydrate at the contacting area, and thus a firm adhering between PDMS and gold would be formed, which led to easy transfer of the gold film when peeled off. The adhesion mechanism can be schematically expressed as Figure 5.

Investigation on treatment conditions and timing further illustrated the mechanism. Without the plasma treatment, the gold film would be hardly adhered and transferred directly by the PDMS stamps, whether they were plasma-treated or not (Figure 6a-1, a-2). When the gold film was treated for even a short time, it would be adhered and peeled off the original chip. More over, with a simultaneously treated PDMS stamp, almost full transfer could be achieved, but with an untreated stamp, only a partial transfer could be made (Figure 6a-3, a-4). The results implied plasma treatment plays an indispensable role in the gold transfer process. It resulted from the generation of $-\text{OH}$ groups on the gold surface, which was essential to react with Si–OH

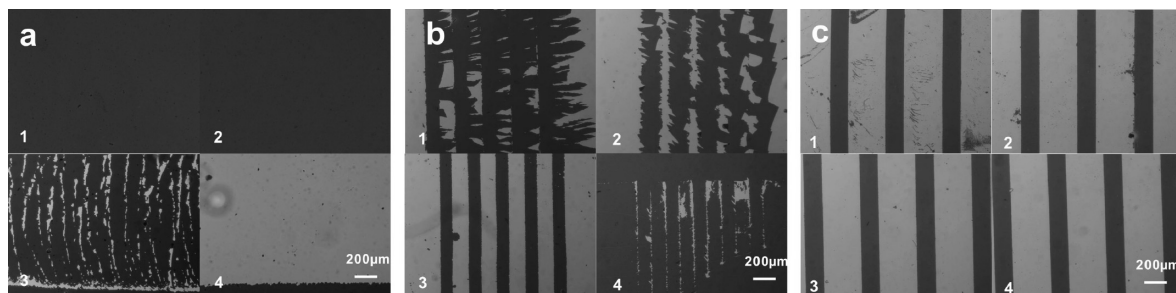


FIGURE 6. Transfer effect under different conditions: (a) transfer (a1, a3) without and (a2, a4) with plasma treatment for PDMS while (a1, a2) without and (a3, a4) with plasma treatment for the gold film; (b) transfer-deprinting for pattern with plasma treated for (b1) 0.5, (b2) 1, (b3) 1.5, and (b4) 2 min; (c) transfer-deprinting for pattern with adhering time of (c1) 1, (c2) 2, (c3) 3, and (c4) 4 min at ambient environment.

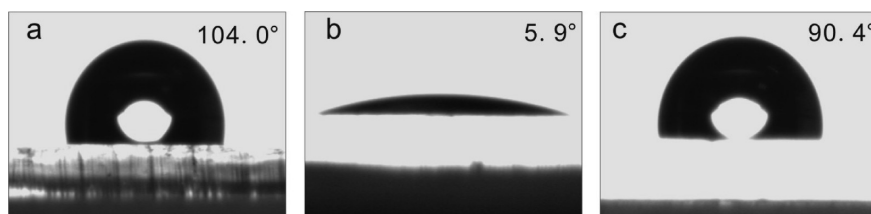


FIGURE 7. Water contact angle (a) before and (b) after plasma treatment, (c) after 2 days of plasma treatment.

groups on PDMS for the conjugation and transfer. And the amount of Si–OH groups on PDMS affects the link strength, which led to different transfer effect by pure PDMS and plasma-treated PDMS. Few Si–OH groups on untreated PDMS made a weak conjugation with gold film, and thus a bad transfer took place. With plasma treated, –OH groups increased by time both on gold and PDMS (36–38), forming a strong enough conjugation and a better transfer. For this reason, the transfer effect would be greatly dependent on the time of plasma treatment. Parallel experiments with different treating time of 0.5, 1, 1.5, 2, and much longer were carried out, and the results showed that when treated for less than 1.5 min, the gold film was transferred badly with a lot of residues. However, although the treating time reaches to 2 min and longer, an obvious decline transfer effect was observed that most of the film could not be adhered and peeled off so easily (Figure 6b). As prospected, enough time of plasma treatment was necessary for a good transfer. But treating too long a time for PDMS would lead to the formation of rough layers of silicon dioxide because of over oxidation, and thus it decreased the amount of –OH groups on surface and prevented the sufficient contact with substrate (39), which was the reason why the transfer became worse when the plasma-treated time exceeded 2 min. More repeated tests showed the best gold film transfer was obtained when plasma-treated for about 100s.

The contact time for adhering also influences the transfer. The transfer effects under 1 min, 2 min, 3 min, 4 min and longer adhering time were compared (Figure 6c). An optimized adhering time is at least 3 min. Less than this time, a few parts of the film would be left on substrate. Longer time with heat-up assisting was found to be of great improvements for the transfer, because they could enforce the dehydration between Au–OH and Si–OH to supply a strong enough conjugation force for the transfer. However, –OH groups on gold surface could not last for long because the fast transformation of Au(OH)_x to AuO_x (24). Therefore,

when exposed in the air for a while purposely, the treated gold film would not be transferred perfectly.

The same reason accounted for the changes of water contact angle before and after plasma treatment to the gold film (Figure 7). Original gold film showed a contact angle of 104° close to pure PDMS substrate, while plasma-treated gold film showed a more hydrophilic property with the contact angle about 5.9°, which resulted from the formation of –OH groups. However, after more than 2 days, the contact angle rebounded to about 90.4°, and it could not recover to exactly the same state as the original film even after several days, which in fact was according with the result in our previous work (24) that AuO_x was formed at last because of the dehydration.

To confirm the transfer mechanism derived from the formation of –OH groups but not the redeposited carbonaceous materials onto the gold during the plasma exposure, electrochemical and XPS results before and after plasma treatment were compared, which were shown in Figures S1 and S2 and Table S1 in the Supporting Information, respectively. If the carbonaceous material contamination onto the gold occurs during the plasma exposure, part of the gold would be covered and the reduction peak current of the gold oxide at 0.65 V(vs Ag/AgCl) in 0.5 M H₂SO₄ would decrease. Here after plasma treatment, the almost same CV as that of gold film before plasma treatment suggests that no any contamination existed on the gold during the plasma exposure (see Figure S1 in the Supporting Information). And the

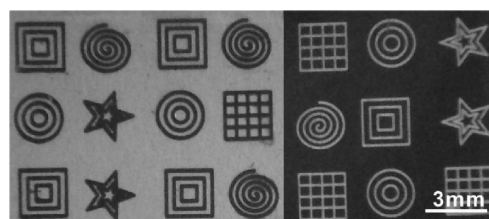


FIGURE 8. Large area of gold patterns and PDMS patterns.

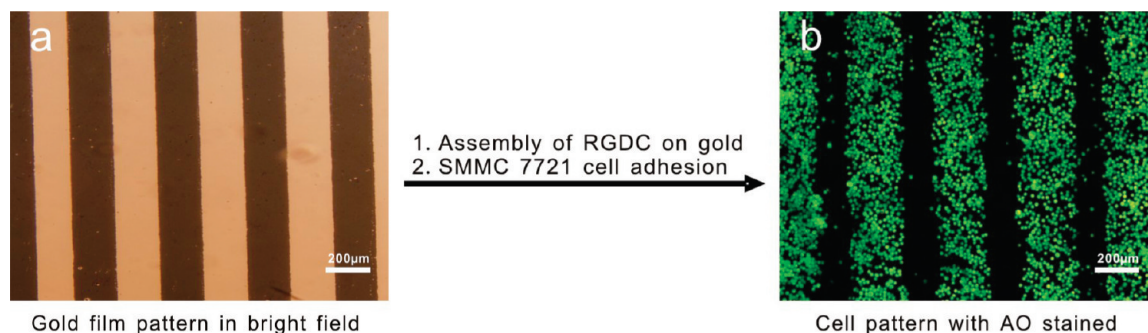


FIGURE 9. Cell patterns with the fabricated gold patterns.

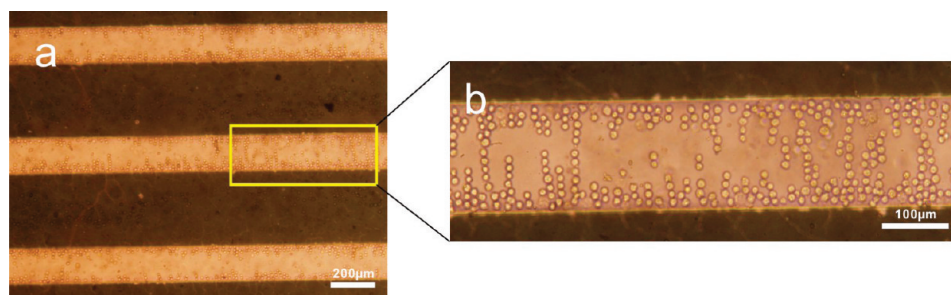


FIGURE 10. Dielectrophoresis control of live HL-60 cells (a) after applying AC voltages for 5 min, and (b) magnified image of the selected area in a.

XPS results of gold film before and after plasma treatment also support this point. After plasma treatment, the ratio of C/Au decreased while the ratio of O/Au increased, which suggested that there was no possible contamination of carbonaceous materials on the surface (see Figure S2 and Table S1 in the Supporting Information).

Pattern Results and Cell Patterning. Using the developed method we could obtain different kinds of gold or PDMS patterns (Figure 8). The whole area of the pattern chip was dependent by the area of the gold film and the stamp. With different kinds of stamps, we could achieve different kinds of patterns even on the same PDMS substrate. Figure 8 showed real photos of the positive gold patterns and negative PDMS patterns obtained by deprinting and printing method, respectively. All the patterns were obtained with 5 min adhering at 60 °C before peeled off.

Cell patterning was often carried out on gold surface for its good biocompatibility and easy SAM-coated. Here, based on the fabricated gold patterns, we used a multi-peptide Arg-Gly-Asp-Cys (RGDC) to self-assemble on the gold surface and to induce cell anchoring for the pattern. RGD peptide is a ligand for several integrin receptors and often acts as a functional group to tailor cell-adhesive surface of patterns and enhance the attachment and growth of cells (40–46). Via the self-assembly of –SH group in cysteine on the gold surface, RGDC peptide was grafted onto the gold patterns. After culture for 2 h in medium supplemented with serum, SMMC7721 cells adhere to the gold patterns grafted with RGDC selectively. Figure 9 shows the whole process from a gold pattern to a cell pattern. The viability of cells immobilized on gold patterns was clearly investigated using AO fluorescence dye (Figure 9b).

Dielectrophoresis Control of Live Cells. The implementation of dielectrophoresis requires patterning of

conductive electrodes for the application of the electric fields, which can be supplied by a rapid pattern approach like above. At the beginning, HL-60 cells dispersed over the chamber, and slowly settled down toward the bottom. When the AC voltage was applied to the interdigital electrodes, cells were polarized and began to align into chains in the direction of the electric field lines. Within 10 min, the manipulated cells showed the typical assembly of pearl chains parallel to the electric fields, and located between the electrodes of the strongest electric field intensity, which resulted from the interaction between the dipoles induced in the cells (Figure 10).

CONCLUSIONS

To conclude, positive gold micropatterns and negative PDMS micropatterns on elastomeric PDMS with large area can be successfully achieved by either deprinting or printing with the microcontact transfer method. And the use of air plasma treatment made the transfer easier without conventional complicated SAM coating. The resulting gold film has quite good electrochemical properties with a smooth surface, which allowed the RGDC SAMs perfect formation and subsequent cell adhesion, as well as the practical applications for the fabrication of the microelectrodes in microfluidics. The attractive merits of this method lie in the availability in ordinary chemistry laboratories without the need of a clean room, metal sputtering facility, and photolithographic procedures. With this method, a lot of lab-on-a-chip systems could be developed conveniently in the future.

Acknowledgment. This work was supported by the National Natural Science Foundation of China (20890021, 20775033), the National Natural Science Funds for Creative Research Groups (20821063), and the 973 Program (2007CB936404, 2006CB933201).

Supporting Information Available: Electrochemical and XPS results before and after plasma treatment for gold film. This material is available free of charge via the Internet at <http://pubs.acs.org>.

REFERENCES AND NOTES

- Xia, Y. N.; Whitesides, G. M. *Annu. Rev. Mater. Sci.* **1998**, *28*, 153–184.
- Wolfe, D. B.; Love, J. C.; Gates, B. D.; Whitesides, G. M.; Conroy, R. S.; Prentiss, M. *Appl. Phys. Lett.* **2004**, *84*, 1623–1625.
- Xia, Y. N.; Mrksich, M.; Kim, E.; Whitesides, G. M. *J. Am. Chem. Soc.* **1995**, *117*, 9576–9577.
- Zhao, D.; Duan, L. T.; Xue, M. Q.; Ni, W.; Cao, T. B. *Angew. Chem., Int. Ed.* **2009**, *48*, 6699–6703.
- Hyun, J.; Zhu, Y. J.; Liebmman-Vinson, A.; Beebe, T. P.; Chilkoti, A. *Langmuir* **2001**, *17*, 6358–6367.
- Buxboim, A.; Geron, E.; Alon, R.; Bar-Ziv, R. *Small* **2009**, *5*, 1723–1726.
- Rogers, J. A.; Bao, Z. N.; Baldwin, K. W.; Dodabalapur, A.; Crone, B.; Raju, V. R.; Kuck, V.; Katz, H. E.; Amundson, K.; Ewing, J.; Drzagic, P. *Proc. Natl. Acad. Sci. U.S.A.* **2001**, *98*, 4835–4840.
- Rogers, J. A. *Science* **2001**, *291*, 1502–1503.
- Briseno, A. L.; Roberts, M.; Ling, M. M.; Moon, H. E.; Nemanick, J.; Bao, Z. N. *J. Am. Chem. Soc.* **2006**, *128*, 3880–3881.
- Loo, Y. L.; Someya, T.; Baldwin, K. W.; Bao, Z. N.; Ho, P.; Dodabalapur, A.; Katz, H. E.; Rogers, J. A. *Proc. Natl. Acad. Sci. U.S.A.* **2002**, *99*, 10252–10256.
- Meitl, M. A.; Zhu, Z. T.; Kumar, V.; Lee, K. J.; Feng, X.; Huang, Y. Y.; Adesida, I.; Nuzzo, R. G.; Rogers, J. A. *Nat. Mater.* **2006**, *5*, 33–38.
- Song, L.; Ci, L. J.; Gao, W.; Ajayan, P. M. *ACS Nano* **2009**, *3*, 1353–1356.
- Kowalczyk, B.; Apodaca, M. M.; Nakanishi, H.; Smoukov, S. K.; Grzybowski, B. A. *Small* **2009**, *5*, 1970–1973.
- Kim, D. H.; Kim, Y. S.; Wu, J.; Liu, Z. J.; Song, J. Z.; Kim, H. S.; Huang, Y. Y.; Hwang, K. C.; Rogers, J. A. *Adv. Mater.* **2009**, *21*, 3703–3707.
- Loo, Y. L.; Willett, R. L.; Baldwin, K. W.; Rogers, J. A. *Appl. Phys. Lett.* **2002**, *81*, 562–564.
- Lee, Y. C.; Chiu, C. Y. *J. Micromech. Microeng.* **2008**, *18* (1–7), 075013.
- Kim, J. W.; Yang, K. Y.; Hong, S. H.; Lee, H. *Appl. Surf. Sci.* **2008**, *254*, 5607–5611.
- Chen, J. Y.; Mela, P.; Möller, M.; Lensen, M. C. *ACS Nano* **2009**, *3*, 1451–1456.
- Loo, Y. L.; Willett, R. L.; Baldwin, K. W.; Rogers, J. A. *J. Am. Chem. Soc.* **2002**, *124*, 7654–7655.
- Loo, Y. L.; Lang, D. V.; Rogers, J. A.; Hsu, J. W. P. *Nano Lett.* **2003**, *3*, 913–917.
- Felmet, K.; Loo, Y. L.; Sun, Y. M. *Appl. Phys. Lett.* **2004**, *85*, 3316–3318.
- Loo, Y. L.; Hsu, J. W. P.; Willett, R. L.; Baldwin, K. W.; West, K. W.; Rogers, J. A. *J. Vac. Sci. Technol., B* **2002**, *20*, 1071–1073.
- Bai, H. J.; Shao, M. L.; Gou, H. L.; Xu, J. J.; Chen, H. Y. *Langmuir* **2009**, *25*, 10402–10407.
- Wu, J.; Bai, H. J.; Zhang, X. B.; Xu, J. J.; Chen, H. Y. *Langmuir* **2010**, *26*, 1191–1198.
- Chen, S. P.; Wu, J.; Xu, J. J.; Chen, H. Y. Unpublished information.
- Gong, J. L.; Mullins, C. B. *Acc. Chem. Res.* **2009**, *42*, 1063–1073.
- Sault, A. G.; Madix, R. J.; Campbell, C. T. *Surf. Sci.* **1986**, *169*, 347–356.
- Kim, T. S.; Gong, J.; Ojifinni, R. A.; White, J. M.; Mullins, C. B. *J. Am. Chem. Soc.* **2006**, *128*, 6282–6283.
- Gong, J. L.; Mullins, C. B. *J. Am. Chem. Soc.* **2008**, *130*, 16458–16459.
- Saliba, N.; Parker, D. H.; Koel, B. E. *Surf. Sci.* **1998**, *410*, 270–282.
- Deng, X. Y.; Friend, C. M. *J. Am. Chem. Soc.* **2005**, *127*, 17178–17179.
- Xu, B. J.; Liu, X. Y.; Haubrich, J.; Madix, R. J.; Friend, C. M. *Angew. Chem., Int. Ed.* **2009**, *48*, 4206–4209.
- Kim, T. S.; Stiehl, J. D.; Reeves, C. T.; Meyer, R. J.; Mullins, C. B. *J. Am. Chem. Soc.* **2003**, *125*, 2018–2019.
- Ojifinni, R. A.; Gong, J. L.; Froemming, N. S.; Flaherty, D. W.; Pan, M.; Henkelman, G.; Mullins, C. B. *J. Am. Chem. Soc.* **2008**, *130*, 11250–11251.
- Quiller, R. G.; Baker, T. A.; Deng, X. Y.; Colling, M. E.; Min, B. K.; Friend, C. M. *J. Chem. Phys.* **2008**, *129* (1–9), 064702.
- Hui, A. Y. N.; Wang, G.; Lin, B.; Chan, W. T. *Lab Chip* **2005**, *5*, 1173–1177.
- Morra, M.; Occhiello, E.; Marola, R.; Garbassi, F.; Humphrey, P.; Johnson, D. *J. Colloid Interface Sci.* **1990**, *137*, 11–24.
- Makamba, H.; Kim, J. H.; Lim, K.; Park, N.; Hahn, J. H. *Electrophoresis* **2003**, *24*, 3607–3619.
- Millare, B.; Thomas, M.; Ferreira, A.; Xu, H.; Holesinger, M.; Vullev, V. I. *Langmuir* **2008**, *24*, 13218–13224.
- Bai, H. J.; Gou, H. L.; Xu, J. J.; Chen, H. Y. *Langmuir* **2010**, *26*, 2924–2929.
- Mrksich, M. *Chem. Soc. Rev.* **2000**, *29*, 267–273.
- Lee, S. H.; Moon, J. J.; West, J. L. *Biomaterials* **2008**, *29*, 2962–2968.
- Yousaf, M. N.; Houseman, B. T.; Mrksich, M. *Proc. Natl. Acad. Sci. U.S.A.* **2001**, *98*, 5992–5996.
- Hahn, M. S.; Miller, J. S.; West, J. L. *Adv. Mater.* **2006**, *18*, 2679–2684.
- Koh, W. G.; Itle, L. J.; Pishko, M. V. *Anal. Chem.* **2003**, *75*, 5783–5789.
- Kalinina, S.; Gliemann, H.; Lopez-Garcia, M.; Petershans, A.; Auernheimer, J.; Schimmel, T.; Bruns, M.; Schambony, A.; Kessler, H.; Wedlich, D. *Biomaterials* **2008**, *29*, 3004–3013.

AM100196Z